J Fluoresc (2015) 25:1013–1021
DOI 10.1007/s10895-015-1585-2

ORIGINAL PAPER

Spectroscopic Studies on Binding of Porphyrin-Phenazine Conjugate to Four-Stranded Poly(G)

Olga Ryazanova[1] · Victor Zozulya[1] · Igor Voloshin[1] · Larysa Dubey[2] · Igor Dubey[2] · Victor Karachevtsev[1]

Received: 17 February 2015 / Accepted: 20 May 2015 / Published online: 16 June 2015

Abstract Binding of a novel cationic porphyrin–imidazophenazine conjugate, $TMPyP^{3+}$–ImPzn, to four-stranded poly(G) was investigated in aqueous solutions of neutral pH under near physiological ionic conditions using absorption, polarized fluorescent spectroscopy and fluorescence titration techniques. In absence of the polymer the conjugate folds into stable internal heterodimer with stacking between the porphyrin and phenazine chromophores. Binding of $TMPyP^{3+}$–ImPzn to poly(G) is realized by two competing ways. At low polymer-to-dye ratio ($P/D<6$) outside electrostatic binding of the cationic porphyrin moieties of the conjugate to anionic polynucleotide backbone with their self-stacking is predominant. It is accompanied by heterodimer dissociation and distancing of phenazine moieties from the polymer. This binding mode is characterized by strong quenching of the conjugate fluorescence. Increase of P/D results in the disintegration of the porphyrin stacks and redistribution of the bound conjugate molecules along the polymer chain. At $P/D>10$ another binding mode becomes dominant, embedding of $TMPyP^{3+}$–ImPzn heterodimers into poly(G) groove as a whole is occurred.

✉ Olga Ryazanova
ryazanova@ilt.kharkov.ua

[1] Department of Molecular Biophysics, B. Verkin Institute for Low Temperature Physics and Engineering, National Academy of Sciences of Ukraine, 47 Lenin ave, 61103 Kharkov, Ukraine

[2] Department of Synthetic Bioregulators, Institute of Molecular Biology and Genetics, National Academy of Sciences of Ukraine, 150 Zabolotnogo str., 03680 Kyiv, Ukraine

Keywords Porphyrin-imidazophenazine conjugate · Poly(G) · G-quadruplex · Polarized fluorescent spectroscopy · Absorption spectroscopy · Binding

Introduction

During last two decades porphyrin derivatives attracted a considerable scientific interest, especially water-soluble cationic *meso*-substituted porphyrins with extended heteroaromatic system. A number of porphyrins of this group, e.g., extensively studied for years 5,10,15,20-tetra-(N-methyl-4-pyridyl)porphine (TMPyP4), were found to be efficient DNA binders [1, 2], photonucleases [3] and agents for photodynamic therapy [4, 5]. Complexes of TMPyP4 and other cationic porphyrins with some Red-Ox-active transition metals (Mn^{3+}, Fe^{3+}, Cu^{2+}, etc.) are able to perform oxidative DNA cleavage [6]. TMPyP4 was also found to be an efficient antitumor agent targeting so called G-quadruplex structures of telomeric DNA [7–9].

Four-stranded DNA structures known as G-quadruplexes, or DNA tetraplexes, have recently emerged as a new therapeutic target for anticancer strategy. G-quadruplexes (G4) are unique DNA arrangements formed by stacked arrays of guanine quartets connected by non-canonical Hoogsteen-type hydrogen bonds. G-quadruplexes were shown to play a crucial biological role. DNA sequences able to fold into G4 structures are prevalent in telomeric DNA, although they have been also found in a number of gene promoter regions, primarily in proto-oncogenes like *c-myc* or *k-ras* [10–12]. Specific binding of a drug to telomeric G4 structures may inhibit the telomerase enzyme expressed in most cancer cells (in contrast to normal

somatic cells) that results in anticancer activity [7–11]. It is interesting to note that in this approach, enzyme inhibition is achieved due to the interaction of ligands with its substrate, telomeric DNA, rather than the enzyme itself.

A number of efficient G-quadruplex binding/stabilizing ligands with anticancer properties have been reported in the literature. They are usually based on planar heteroaromatic systems like acridines, anthraquinones, carbazoles, macrocyclic polyoxazoles, etc. [7–9].

G-quartet consists of four guanine bases, so its square is twice as large as the square of the base pair. Due to this large area of G-quartet, an efficient and specific quadruplex binder should have a large aromatic or heteroaromatic surface, larger than that required for duplex ligands, to provide an efficient π-π-interaction with its molecular target [8, 9]. From this point of view, large porphyrin chromophores may be ideal G4 ligands as their molecules perfectly overlap with G-quartets.

Indeed, a number of cationic porphyrins, first of all TMPyP4, were identified as efficient G4 ligands and telomerase inhibitors. At the same time, porphyrin conjugation to other molecules can affect ligand binding further stabilizing G-quadruplex structure that can increase antitumor activity. However, chemical attachment of other molecular fragments to TMPyP4 is difficult. On the other hand, its tricationic analog $TMPyP^{3+}$ can be easily functionalized, e.g., by introducing the carboxylic function or amino group, and thus is suitable for the conjugation to other molecules.

In recent years, $TMPyP^{3+}$ porphyrin was covalently attached to a number of molecules, including oligonucleotides to achieve site-specific DNA cleavage or modification [13–15], peptides [16], a number of ligands to obtain efficient DNA photocleavage and photocytotoxic agents, including acridine [17], anthraquinone [18], phenylpiperazine [19], β-carboline [20], EDTA [21], C_{60} fullerene for molecular photoelectrochemical devices [22], etc. In these cases $TMPyP^{3+}$ derivatives were directed against duplex or single-stranded DNA. At the same time, there are several reports in the literature concerning the synthesis and study of cationic porphyrin conjugates with other ligands aimed at improving the binding affinity to G-quadruplex DNA and its stabilization. These compounds include e.g., aminoquinoline [23] and anthraquinone [24] conjugates of $TMPyP^{3+}$.

To achieve this goal we have attached $TMPyP^{3+}$ to imidazophenazine dye (ImPzn) via carboxyalkyl linker (Fig. 1) [25]. Imidazophenazine is known as DNA intercalator [26, 27], and we supposed that the attached dye would improve the binding of porphyrin to G4 structures by intercalation into double-stranded regions of telomeric DNA or between guanine quartets. Indeed, $TMPyP^{3+}$–imidazophenazine hybrids and their zinc(II) and manganese(III) complexes efficiently inhibited telomerase and demonstrated antiproliferative activity in vitro at micro- and submicromolar concentrations [28].

The binding of this porphyrin–imidazophenazine conjugate and its metalocomplexes with intramolecular G-quadruplex formed by 5'-d[AGGG(TTAGGG)$_3$]-3' 22-mer oligodeoxynucleotide of human telomeric repeat (Tel22, PDB code 143D) has been studied using spectroscopic techniques. It was shown that the metaloconjugate stabilizes the abovementioned quadruplex [29].

At the same time, it is known that G-quadruplexes are highly polymorphic DNA and RNA arrangements. There are intra- and intermolecular quadruplexes, with parallel, antiparallel and hybrid-type G4 structures [9, 11, 30, 31]. For example, 22-mer oligonucleotide Tel22 forms a parallel type intramolecular G-quadruplex in the presence of K^+ ions [32]. In the present study, we have used a polyguanylic acid [poly(G)] known to form a strong self-structure [33] as a model system to investigate the binding of porphyrin-imidazophenazine conjugate. The study of the ligand binding to poly(G) is of great interest as this polynucleotide is capable to form telomere-like structure. Poly(G) and poly(dG) are known to form four-stranded helical arrangements with the G-tetrads stacked on one another [31, 34]. Thus poly(G) is suitable for the modelling of G-quadruplex regions of telomeric DNA and ligand-quadruplex interactions.

The aim of present work is registration and analysis of spectroscopic changes in absorption and fluorescence properties of the cationic porphyrin – imidazophenazine conjugate induced by its binding to long four-stranded poly(G) polymer at different polymer-to-dye ratios.

Materials and Methods

Chemicals

$TMPyP^{3+}$–ImPzn conjugate (Fig. 1) were synthesized and purified by the procedures described in [25]. Briefly, tris(4-pyridyl)phenylporphine containing a carboxybutyl function [35] was conjugated to N_1-aminoalkyl derivative of imidazo[4,5-b]phenazine in the presence of BOP-HOBT coupling reagent, followed by N-methylation of pyridine residues by methyl iodide. Imidazo[4,5-b]phenazine dye and its aminoalkyl derivatives were obtained in accordance with methods reported in [36]. Poly(G) polynucleotide from Sigma Chem. Co. were used as received.

The 2 mM phosphate buffer (pH6.9) containing 0.5 mM EDTA and 0.1 M NaCl, prepared from deionized water, was used as a solvent.

The concentration of the conjugate was determined gravimetrically. The concentration of the poly(G) polynucleotide was determined spectrophotometrically in aqueous solution using the extinction value ε_{252}=9900 M^{-1} cm^{-1} at room temperature. The formation of four-stranded structure was proved by melting experiments with the registration of the

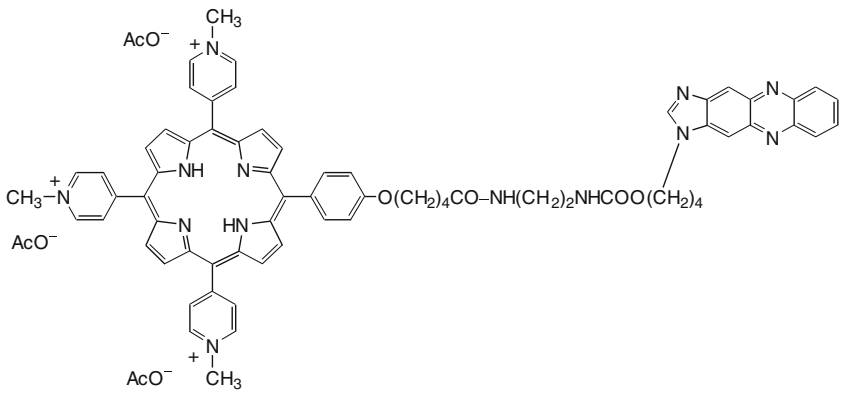

Fig. 1 Molecular structure of porphyrin–imidazophenazine conjugate ($TMPyP^{3+}$–ImPzn)

temperature dependence of polymer absorbance at 295 nm in accordance with the procedure [37].

Apparatus and Techniques

The spectroscopic properties of free $TMPyP^{3+}$–ImPzn conjugate (Fig. 1) and its complexes with four-stranded poly(G) have been studied using absorption and polarized fluorescent spectroscopy techniques.

Electronic absorption spectra in the visible range were recorded on SPECORD UV/VIS spectrophotometer (Carl Zeiss, Jena). Fluorescent measurements were carried out on laboratory spectrofluorimeter based on the DFS-12 monochromator (LOMO, 350–800 nm range, dispersion 5 Å/mm) by the method of photon counting [38]. The fluorescence was excited by the stabilized linearly polarized radiation of a halogen lamp, at λ_{exc}=440 and 530 nm. The emission was observed at an angle of 90° from the excitation beam. The fluorescence polarization degree, p, has been calculated from the equation [39]:

$$p = \frac{I_{II} - I_{\perp}}{I_{II} + I_{\perp}} \quad (1)$$

where I_{II} and $I_{\perp}$ are intensities of the emitted light, which are polarized parallel and perpendicular to the polarization direction of exciting light, respectively. Fluorescence spectra were corrected on the spectral sensitivity of the spectrofluorimeter.

Relative quantum yield of the fluorescence was calculated from the equation

$$\frac{Q}{Q_0} = \frac{F_S}{F_{S0}} \cdot \frac{A_0}{A} \quad (2)$$

where F_{S0} and F_S are integral intensities of the conjugate fluorescence in the free state and in the mixture with poly(G), respectively, which are calculated as areas under the corresponding fluorescence spectra; A_0 and A are the absorbances of these samples under λ_{exc}.

The spectroscopic experiments were carried out in quartz cells at room temperature from 20 to 22 °C.

To obtain the dependencies of the fluorescence intensity and polarization degree for porphyrin and phenazine moieties of the conjugate on the molar polymer-to-dye ratio, P/D, the series of fluorescence titration experiments were performed. Here the conjugate sample was added with increasing amounts of the concentrated poly(G) stock solution containing the same conjugate content of 10 μM to achieve the desired P/D value in the final solution, whereas fluorescence intensity and polarization degree were measured at λ_{obs}=562 and 670 nm, excitation wavelength was λ_{exc}=440 nm. The time from 7 to 10 min was required to reach the thermodynamic equilibrium in the system which was verified from the stability in the fluorescence signal.

Results

Absorption and fluorescence spectra of $TMPyP^{3+}$–ImPzn conjugate

Electronic absorption and fluorescence spectra of free $TMPyP^{3+}$–ImPzn conjugate as well as of individual $TMPyP^{3+}$ and ImPzn dyes are presented in Figs. 2 and 3. It can be seen that visible $TMPyP^{3+}$ absorption spectrum (Fig. 2) consists of intense Soret band at 425.5 nm (extinction *ca.* 200,000 M^{-1} cm^{-1}) and four less intense Q-bands centered at 522, 561, 583.5 and 642.5 nm [29]. Its shape is similar to the spectrum of tetracationic TMPyP4 porphyrin [38], however small red shift (*ca.* 3 nm) of all bands is observed. The absorption of individual ImPzn dye is characterized by the intense shortwave band at 385 nm (extinction *ca.* 16,300 M^{-1} cm^{-1}) and the broad longwave shoulder extending to 490 nm [40]. $TMPyP^{3+}$ fluorescence spectrum (Fig. 3) is typical for free base porphyrins. It consists of one wide stuctureless band centered at *ca.* 717 nm, which fluorescence polarization degree, p, is around of 0.015. ImPzn emission band has a maximum at 562 nm (Fig. 3), $p \approx 0.015$ [40].

Absorption spectrum of $TMPyP^{3+}$–ImPzn conjugate (Fig. 2) represents a superposition of $TMPyP^{3+}$and ImPzn

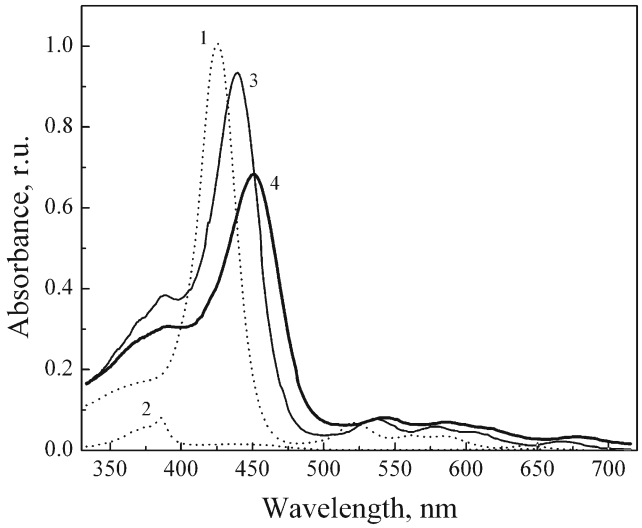

Fig. 2 Absorption spectra of individual $TMPyP^{3+}$ (**1**) and ImPzn (**2**) dyes, free $TMPyP^{3+}$–ImPzn (**3**) and $TMPyP^{3+}$–ImPzn conjugate bound to poly(G) at P/D=115 (**4**). The measurements were carried out in 2 mM phosphate buffer pH6.9 containing 0.5 mM EDTA and 0.1 M NaCl. Ligand concentration C=10 μM, path length=0.5 cm

spectra [29]. Though, conjunction of the dyes results in near 10 % hypochromism and 10 nm red shift of $TMPyP^{3+}$ Soret peak (up to 435 nm), more than 5-fold quenching of the porphyrin emission, splitting of the fluorescence spectrum into two distinct bands with maxima at 673 and 729 nm (Fig. 3), insignificant decrease of fluorescence polarization degree (up to 0.01). Also, strong 50-fold fluorescence quenching was registered for the phenazine moiety, which can be explained by the non-radiative Förster resonance energy heterotransfer (FRET) from phenazine part of hybrid to porphyrin one, since substantial overlapping of porphyrin absorption band $Q_y(0,0)$

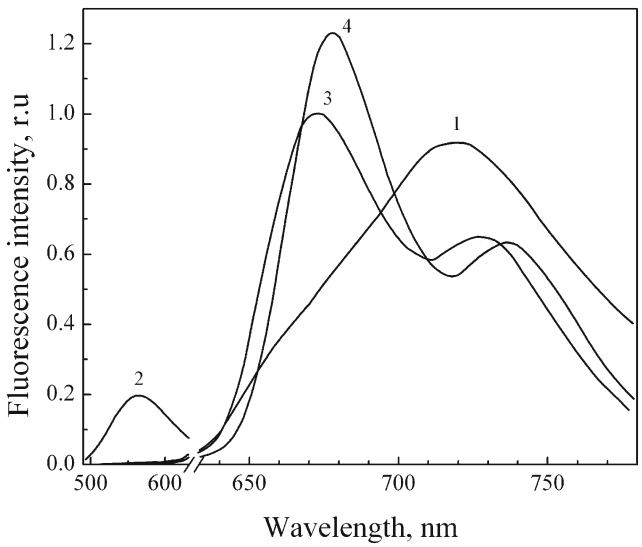

Fig. 3 Normalized fluorescence spectra of free $TMPyP^{3+}$ (**1**) and ImPzn (**2**) (both spectra are reduced by five times), $TMPyP^{3+}$–ImPzn conjugate in a free state (**3**) and bound to poly(G) at P/D=115 (**4**). The fluorescence was excited at λ_{exc}=530 nm. Experimental conditions as in Fig. 2

(λ_{max}=561 nm) and ImPzn emission one (λ_{max}=562 nm) is occurred. As it is known, the efficiency of FRET is very sensitive to changes in the distances between donor and acceptor chromophores (inversely proportional to the sixth power of the interchromophore distance), to the spectral overlap of the donor emission and the acceptor absorption spectra, as well as to the relative orientation of the donor emission and the acceptor absorption dipole moments [39]. Thereby strong quenching of ImPzn fluorescence indicates the close proximity of its chromophore to the acceptor (porphyrin). Spectral properties of $TMPyP^{3+}$ and ImPzn alone as well as $TMPyP^{3+}$–ImPzn conjugate are summarised in Table 1.

It is known that emission spectra of the free base porphyrins usually consist of two overlapping bands [41, 42] which can degenerate into one. In particular, it is observed for TMPyP4 porphyrin and its derivatives, whose fluorescence spectra in water represent single structureless bands, which splits in non-polar solvents [43], upon the dimer or stack formation [38], and upon intercalation to DNA [44], when overlapping between the π-electronic systems of neighbouring chromophores or chromophore and bases is occurred. Since at the concentration of 10 μM, the $TMPyP^{3+}$ porphyrin is mainly in monomeric form, it can be assumed that the aforementioned spectral transformations, as well as FRET quenching of ImPzn fluorescence most likely indicate the formation of internal heterodimer where π-staking interaction between $TMPyP^{3+}$ and ImPzn chromophores is occurred [29]. Heating of the conjugate till 95 °C has not revealed any substantial changes in the emission of ImPzn moiety. The fluorescent melting curve represents straight line with only 1.4 –fold rise of ImPzn emission in the end of melting (not shown), that indicates high stability of the dimer formed. Possible structure of the heterodimer was calculated earlier using DFT method together with total and free Gibbs energy of their formation [25].

Fluorescent titration study of $TMPyP^{3+}$–ImPzn + poly(G)

To follow binding of charged porphyrin–phenazine conjugate to long intermolecular quadruplex formed by synthetic poly(G) fluorescence titration experiments were performed, where changes in the relative fluorescence intensity, I/I_0, and polarization degree, p, of the conjugate on molar polymer-to-dye ratio, P/D, were registered near the emission band maxima of both porphyrin and phenazine moiety, at 670 and 562 nm respectively (Fig. 4).

As can bee seen from this figure, both titration curves showing dependence I/I_0 *vs* P/D are biphasic. In the initial descending part of fluorescent titration curve (P/D=0 ÷ 5) registered for $TMPyP^{3+}$–ImPzn hybrid in maximum of porphyrin emission (at λ_{obs}=670 nm) quenching of porphyrin fluorescence is observed with simultaneous rise of fluorescence polarisation degree. At P/D=5÷6 the minimal emission level of ~20 % from initial is registered. And in the range of higher P/D values gradual

Table 1 Spectral properties of individual $TMPyP^{3+}$ and ImPzn dyes, $TMPyP^{3+}$–ImPzn conjugate in a free state and bound to poly(G) measured in the 2 mM phosphate buffer (pH6.9) containing 0.5 mM EDTA and 0.1 M NaCl

Compound	Visible absorption band maxima [a] (nm)	Fluorescence band maxima (nm)	Relative quantum yield of fluorescence [b] Q/Q_0	Normalized fluorescence intensity [c] I/I_0	Fluorescence polarization degree p
$TMPyP^{3+}$	Soret band: 425.5 Q-bands: 522, 561, 583.5, 642.5	717	5.4	–	0.015
ImPzn	385	562	–	–	0.015
$TMPyP^{3+}$–ImPzn	435	673, 729	1	1	0.01
$TMPyP^{3+}$–ImPzn+poly(G) (P/D=115)	446	678, 738	1.01	1.3	0.1
$TMPyP^{3+}$	425.5	717	5.4	1	0.015
$TMPyP^{3+}$ + poly(G) (P/D=115)	446	679, 738	12.4	3.7 [d]	0.095

[a] For the conjugate and its complex with poly(G) only position of Soret band maximum is presented

[b] Values are calculated from the spectra (Fig. 3) according Eq. 2 taking into account the change in absorbance at λ_{exc}=530 nm where A_0/A=0.95

[c] Values are determined at λ_{exc}=440 nm, λ_{obs}=670 nm

[d] Calculated at P/D=115, λ_{exc}=530 nm, λ_{obs}=670 nm

enhancement of porphyrin emission is occurred reaching at P/D=115 magnitude of I/I_0=1.3. For phenazine part of hybrid (λ_{obs}=562 nm) absolutely opposite behavior is observed in the initial part of the fluorescent titration curve. Here intensity of ImPzn emission almost linearly increases up to $I/I_o \approx 2$ at P/D=4.5. Then, in the range of P/D from 4.5 to 9, it somewhat quenches, and further polymer addition again induces the gradual rise of the dye fluorescence, which at P/D=115 reaches value of $I/I_o \approx 2.35$. Fluorescence polarization degree, p, measured for both conjugate moieties also increases during the binding process (see inset of Fig. 4). At high P/D values it reaches level of 0.1 for the porphyrin moiety, and 0.05 for the phenazine one. Unfortunately, low level of almost quenched phenazine emission (approximately 60 cps in the ImPzn band maximum) reduces the accuracy of its magnitude determination.

Absorption and fluorescence spectra of $TMPyP^{3+}$–ImPzn conjugate bound to poly(G)

To show spectral transformations occurred as a result of the conjugate binding to long quadruple poly(G), visible absorption and fluorescence spectra were recorded for complex with high polymer content (P/D>100) (Figs. 2 and 3). The fluorescence was excited at λ_{exc}=530 nm where absorption of the free conjugate and their complexes with poly(G) are practically equal (maximal difference does not exceed 5 % of measured value). The relative quantum yield of the fluorescence was calculated according Eq. 2 and summarized in Table 1.

It is seen that binding of $TMPyP^{3+}$– ImPzn to poly(G) results in 11 nm red shift and substantial hypochromism of its absorption spectrum (*ca.* 17 % in the porpyrin Soret band, see Fig. 2) as well as approximately 1.2-fold increase in the maximum emission intensity (Fig. 3). Maxima of splitted fluorescence band somewhat shift toward longer wavelengths (to 678 and 738 nm). So that Soret band of the bound hybrid is *ca.* 20 nm shifted in comparison with that for the free porphyrin.

Discussion

We have analyzed fluorescent titration curves presented in Fig. 4. In the initial point of the titration (P/D=0) the conjugate molecules are folded into stable internal heterodimer with π-π stacking between porphyrin and phenazine parts [29]. Gradual addition of the polymer induces the opposite changes in fluorescent behavior of porphyrin and phenazine moieties (λ_{obs}=670 and 562 nm respectively). We observe strong fluorescence quenching in the first case, and its enhancement in the later, that indicates dissociation of the heterodimers. Initial descending part of the titration curve (P/D=0 ÷ 5) registered at 670 nm for $TMPyP^{3+}$ moiety is typical for cooperative outside binding of the cationic dyes to linear polyanions with self-stacking of neighboring chromophores [45–47]. In this way, 5-fold fluorescence quenching with simultaneous increase of p can be explained by formation of porphyrin stacks on polyanionic matrix of poly(G) as a result of neutralization of positive charges localized on methylpyridil groups of porphyrins by negatively charged phosphate groups of poly(G). The deviation of the titration curve from a linear form which was observed earlier for pure electrostatic binding of $TMPyP^{3+}$ to inorganic polyphosphate (PPS) [38] confirms that

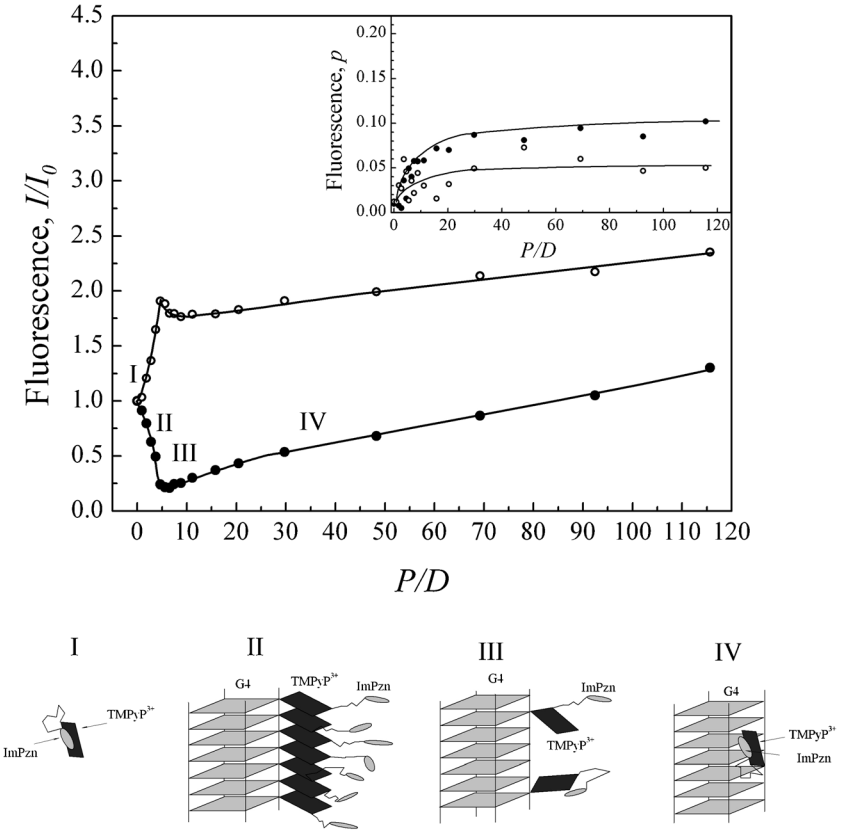

Fig. 4 Dependence of normalized fluorescence intensity and polarization degree (on the inset) on molar polymer-to-dye ratio, *P*/*D*, registered for $TMPyP^{3+}$–ImPzn + poly(G) complex near the maximum of $TMPyP^{3+}$ fluorescence band, λ_{obs}=670 nm (●) and ImPzn one, λ_{obs}=562 nm (○). Measurements were carried out in phosphate buffer (2 mM Na^+), ligand concentration is 10 μM, λ_{exc}=440 nm. Below pictorial diagram is presented showing complexes of $TMPyP^{3+}$–ImPzn conjugate with four stranded poly(G) formed presumably at different *P*/*D* ratios, where porphyrin – imidazophenazine heterodimers are initially formed in solutions without the polymer at *P*/*D*=0 (I); the heterodimers disintegrates and porphyrin moieties bounds electrostatically to anionic polyG backbone with their self-stacking (II); bound porphyrin stacks disintegrate, the conjugate molecules redistribute along the polymer (III) and they fold into the heterodimers again which incorporate into poly(G) groove as a whole (IV)

dissociation of the heterodimers occurs upon binding process. The symmetrically ascending part of titration curve registered for the ImPzn moiety at 562 nm in the same *P*/*D* range obviously indicate the reduction of energy transfer from phenazine part to porphyrin as a result of the dimer dissociation. Emission of phenazine part at *P*/*D*=4.5 is doubled in comparison with that at *P*/*D*=0, however its level registered for individual ImPzn dye is not reached. It is suggested that phenazine moieties of the conjugate are distanced both from porphyrin parts and from the polymer and they can form stacks too.

The minimal level of the conjugate emission registered in porphyrin part lies at approximately *P*/*D*=6 (Fig. 5), that corresponds to twice as high polymer concentration than that (*P*/*D*≈3) registered for individual $TMPyP^{3+}$ dye bound to poly(G) and PPS. Its magnitude, $(I/I_0)_{min}$=0.2, is equal to that observed for $TMPyP^{3+}$ stacks on PPS matrix [38].

In such a way, the first binding mode predominating at low *P*/*D* values (*P*/*D*<6) can be identified as outside electrostatic binding of the porphyrin parts of the conjugates to poly(G) with their self-stacking. At that heterodimers are dissociated, and phenazine moieties are presumably distanced from the polymer; they can form stacks or to be randomly distributed. Taking into account existence of 4 negative charges localized on the phosphate groups of each G-quartet and 3 positive charges localized on each porphyrin moiety of the conjugate, the integration of several neighboring four-stranded poly(G) chains and porphyrin stacks into the aggregate can be assumed in this *P*/*D* range.

The initial part of the titration curve registered at 670 nm (Fig. 4) have been compared with another curves (Fig. 5) obtained under the same experimental conditions for the same conjugate bound to 5'-d[AGGG(TTAGGG)$_3$]-3' oligomer of human telomeric repeat (22G4) [29], as well as for individual $TMPyP^{3+}$ porphyrin bound to 22G4 [29] and to poly(G) (unpublished data). It was found that the shape of fluorescent titration curves obtained for individual $TMPyP^{3+}$ bound to poly(G) and to short 22G4 oligomer are substantially different. In the case of $TMPyP^{3+}$ + 22G4 system we observe monotonically increasing curve without minimum (Fig. 5). Whereas for $TMPyP^{3+}$ + poly(G) the titration curve is linearly descending, the porphyrin fluorescence quenches up to 43 %

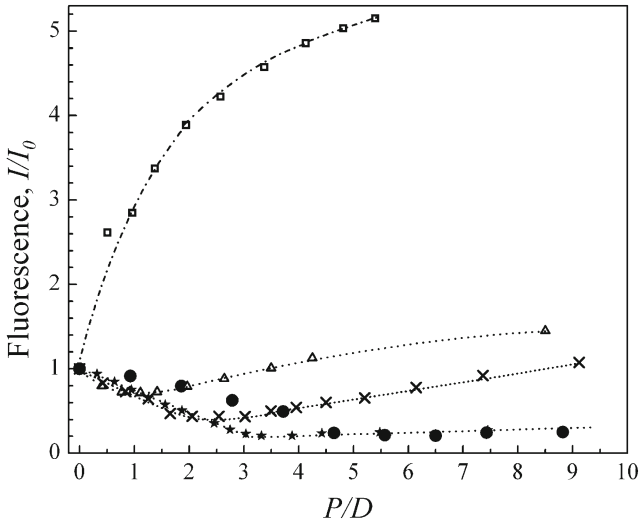

Fig. 5 Comparison of fluorescent titration curves (initial region) registered as dependence of normalized porphyrin emission intensity on molar polymer/dye ratio (*P*/*D*) for tricationic porphyrin and porphyrin-phenazine conjugate bound to long quadruplexes formed by poly(G) and short one formed by 22-mer oligonucleotide 5'-d[AGGG(TTAGGG)$_3$]-3' of human telomeric repeat (22G4) [29]: TMPyP^{3+}–ImPzn + poly(G) (●), TMPyP^{3+} + poly(G) (✖), TMPyP^{3+} + 22G4 (□), TMPyP^{3+} + PPS (⋆), and TMPyP^{3+}–ImPzn+22G4 (Δ). Measurements were carried out in phosphate buffer (2 mM Na^+), ligand concentration is 10 μM, λ_{exc}=440 nm, λ_{obs}=670 nm

from initial. Such behavior can be explained by a significant difference in the length of these polymers. Since in short 22G4 only 3 guanine tetrads can be formed under the folding, formation of long porphyrin stacks as results of the outside electrostatic binding of the dye to the oligomer is impossible and the fluorescence was not quenched. The curve for TMPyP^{3+}–ImPzn conjugate+22G4 has minimum near *P*/*D*=1.5 where emission is quenched only up to 73 %.

In *P*/*D* range from 6 to 10 we observe small local quenching of the conjugate emission registered in ImPzn part at 562 nm. And after *P*/*D*=10 increase of relative poly(G) content results in the gradual enhancement of emission in both branches of fluorescent titration curves, as well as increase in fluorescence polarization degree which achieves the constant level (Fig. 4). At *P*/*D*=115 magnitude of I/I_0 reaches=1.3 for porphyrin and 2.35 for phenazine moiety. The relative quantum yield of the fluorescence calculated from the spectra (Fig. 3) recorded at *P*/*D*=115 and *P*/*D*=0 according with Eq.2, shows practically negligible change in the integral emission of the conjugate upon its binding to poly(G): Q/Q_0=1.01, though the shape and position of fluorescence band maxima in these both cases are substantially different.

It can be noted that contribution of ImPzn part to the total conjugate emission is more than two orders of magnitude less than that of TMPyP^{3+} moiety, and ImPzn fluorescence band is practically invisible in the conjugate fluorescence spectrum. Therefore effects actually observed in fluorescence spectra upon the conjugate binding are conditioned mainly by behavior of the porphyrin moiety (Fig. 4, λ_{obs}=670).

Absorption and fluorescence spectra of TMPyP^{3+}–ImPzn bound to poly(G) at high *P*/*D* (Figs. 2 and 3) have been compared with those for TMPyP^{3+} bound to poly(G) (unpublished data) at the similar experimental conditions, and for the same conjugate bound to PPS [38] which characterize externally bound to PPS porphyrin monomers or dimers. It was found that the maxima of Soret absorption and fluorescence band for TMPyP^{3+}–ImPzn+poly(G) at *P*/*D*=115 are 15 nm red shifted in comparison with those for TMPyP^{3+}–ImPzn+PPS [38]. At the same time the shape of absorption and fluorescence bands and position of their maxima for TMPyP^{3+}–ImPzn+poly(G) at *P*/*D*=115 are coincident with those for TMPyP^{3+} + poly(G). Binding of individual TMPyP^{3+} dye to poly(G) results in 3.9-fold increase of porphyrin emission (unpublished data), whereas in the case of TMPyP^{3+}–ImPzn+poly(G) only 1.3-fold rise of fluorescence was observed. From analysis of abovementioned information we can suggest that at high *P*/*D* values porphyrin stacks are disintegrated, the conjugate molecules fold into heterodimers redistributing along the polymer and presumably, embedding into the groove of four-stranded poly(G) as a whole. This assumption is supported by 17 % hypochromism and 10 nm shift of absorption spectra registered for TMPyP^{3+}–ImPzn+poly(G) at *P*/*D*=115 in comparison with that for the free conjugate, as well as the rise of *p* up to 0.1. The magnitudes of absorption hypochromism, spectral shifts and *p* registered during the conjugate binding are not big enough to characterize intercalation binding mode [48], but they are sufficient for groove binding. Increase in porphyrin fluorescence observed at high *P*/*D* can be explained by the chromophore dehydratation.

The magnitude of ImPzn emission (Fig. 4, the curve registered at 562 nm) registered upon the conjugate binding to poly(G) at high *P*/*D* can be the cumulative effect of two simultaneous processes: (i) the changes in the efficiency of energy transfer from phenazine moiety to porphyrin one as a result of changes in the distance between their chromophores and/or mutual orientation of the transition dipole moments, and (ii) the quenching of phenazine fluorescence by guanine bases occurred through the photoinduced electron transfer between phenazine in the first singlet excited state and guanine in the ground state which occurs through close contact of the dye and guanine bases [47].

In such a way, analysis of spectroscopic changes accompanying binding of TMPyP^{3+}–ImPzn to poly(G) indicate that both porphyrin and phenazine moieties of the conjugate bind to intermolecular G-quadruplexes formed by poly(G) polynucleotide.

Conclusions

Binding of the TMPyP^{3+}–ImPzn conjugate to four-stranded poly(G) polynucleotide has been studied in aqueous buffered solutions of neutral pH under near physiological ionic

conditions using the techniques of absorption and polarized fluorescent spectroscopy, as well as fluorescence titration. Spectroscopic changes indicate that both porphyrin and phenazine moiety of the conjugate binds to poly(G), and two competitive binding modes are identified.

In the absence of the polymer, $TMPyP^{3+}$–ImPzn conjugate folds into stable intramolecular heterodimer with π-π stacking between porphyrin and phenazine parts. At low *P*/*D* values, the heterodimers are presumably disintegrated, and outside electrostatic binding of positively charged porphyrin moieties to anionic polynucleotide backbone with their self-stacking are predominant, which is characterized by 5-fold quenching of porphyrin and enhancement of phenazine emission. At $P/D>6$, porphyrin stacks are disintegrated, the conjugate molecules redistribute along the polymer, and presumably fold into the heterodimer again which incorporate into poly(G) groove as a whole. Embedding of $TMPyP^{3+}$–ImPzn dimers into poly(G) groove is characterized by significant red shift and hypochromism of the Soret absorption band, moderate red shift and enhancement of the conjugate emission as well as rise of the fluorescence polarization degree. Moderate value of fluorescence polarization degree registered for ImPzn moiety at high *P*/*D* indicates that phenazine molecules are not intercalated into quadruple chain, and they, most likely, embed into the polymer groove along with $TMPyP^{3+}$ part.

Our research has shown that the use of charged conjugate of two organic dyes having different absorption and fluorescence spectra gives additional possibilities to study both energy transfer between them and to observe several binding modes of the conjugate to oppositely charged biopolymers. Moreover, by varying the environmental conditions, in particularly *P*/*D* ratio, we can control the mechanism of the conjugate binding to anionic biopolymer and to manage the energy transfer between adjacent porphyrin molecules, which is observed in continuous porphyrin stacks. The results obtained can be used in nanoelectronics, in particular when creating the structures for photovoltaic cells and in light-harvesting systems.

Acknowledgments This work was partially supported by the NAS of Ukraine program "Fundamental basics of molecular and cell biotechnologies" (grant 43/10)

Compliance with Ethical Standards The authors declare that our manuscript complies with the all Ethical Rules applicable for this journal and that there are no conflicts of interests.

References

1. Munson BR, Fiel RJ (1992) Nucleic Acids Res 20(6):1315–1319
2. Sehlstedt U, Kim SK, Carter P, Goodisman J, Vollano JF, Norden B, Dabrowiak JC (1994) Biochemistry 33(2):417–426
3. Da Ros T, Spalluto G, Boutorine AS, Bensasson RV, Prato M (2001) Curr Pharm Des 7(17):1781–1821
4. O'Connor AE, Gallagher WM, Byrne AT (2009) Photochem Photobiol 85(5):1053–1074
5. Ormond AB, Freeman HS (2013) Materials 6(3):817–840
6. Pitié M, Boldron C, Pratviel G (2006) Adv Inorg Chem 58:77–130
7. De Cian A, Lacroix L, Douarre C, Temime-Smaali N, Trentesaux C, Riou J-F, Mergny J-L (2008) Biochimie 90(1):131–155
8. Monchaud D, Teulade-Fichou M-P (2008) Org Biomol Chem 6(4): 627–636
9. Xu Y (2011) Chem Soc Rev 40(5):2719–2740
10. Balasubramanian S, Neidle S (2009) Curr Opin Chem Biol 13(3): 345–353
11. Collie GW, Parkinson GN (2011) Chem Soc Rev 40(12):5867–5892
12. Duchler M (2012) J Drug Target 20(5):389–400
13. Mestre B, Pratviel G, Meunier B (1995) Bioconjug Chem 6(4): 466–472
14. Li H, Fedorova OS, Trumble RW, Flechter TR (1997) Bioconjug Chem 8(1):49–56
15. Dubey I, Pratviel G, Meunier B (2000) J Chem Soc Perkin Trans 1: 3088–3095
16. Mezo G, Herenyi L, Habdas J, Majer Z, Mysliwa-Kurdziel B, Toth K, Csik G (2011) Biophys Chem 155(1):36–44
17. Ishikawa Y, Yamashita A, Uno T (2001) Chem Pharm Bull 49(3): 287–293
18. Zhao P, Hu L-C, Huang J-W, Zheng K-C, Liu J, Yu H-C, Ji L-N (2008) Biophys Chem 134(1–2):72–83
19. Jia T, Jiang Z-X, Wang K, Li Z-Y (2006) Biophys Chem 119(3): 295–302
20. Kumar D, Mishra BA, Shekar KPC, Kumar A, Akamatsu K, Kusaka E, Ito T (2013) Chem Commun 49(7):683–685
21. Schwach G, Thamyongkit P, Reith LM, Svejda B, Knor G, Pfragner R, Schoefberger W (2012) Bioorg Chem 40:108–113
22. Marczak R, Sgobba V, Kutner W, Gadde S, D'Souza F, Guldi DM (2007) Langmuir 23(4):1917–1923
23. Dixon IM, Lopez F, Esteve J-P, Tejera AM, Blasco MA, Pratviel G, Meunier B (2005) ChemBioChem 6(1):123–132
24. Zhao P, Hu L-C, Huang J-W, Fu D, Yu H-C, Ji L-N (2009) Dyes Pigments 83(1):81–87
25. Dubey LV, Ilchenko MM, Zozulya VN, Ryazanova OA, Pogrebnoy PV, Dubey IY (2011) Int Rev Biophys Chem 2(4):147–152
26. Zozulya V, Blagoi Y, Dubey I, Fedoryak D, Makitruk V, Ryazanova O, Shcherbakova A (2003) Biopolym (Biospectrosc) 72(4):264–273
27. Ryazanova O, Dubey L, Dubey I, Zozulya V (2012) J Fluoresc 22(6):1431–1439
28. Negrutska VV, Dubey LV, Ilchenko MM, Dubey IY (2013) Biopolym Cell 29(3):169–176
29. Zozulya VN, Ryazanova OA, Voloshin IM, Dubey LV, Dubey IY (2011) Int Rev Biophys Chem 2(4):112–119
30. Dai J, Carver M, Yang D (2008) Biochimie 90(8):1172–1183
31. Burge S, Parkinson GN, Hazel P, Todd AK, Neidle S (2006) Nucleic Acids Res 34(19):5402–5415
32. Parkinson GN, Lee MP, Neidle S (2002) Nature 417:876–880
33. Pochon F, Michelson AM (1965) Proc Natl Acad Sci USA 53: 1425–1430
34. Howard FB, Frazier J, Miles HT (1977) Biopolymers 16(4):791–809
35. Casas C, Saint-Jalmes B, Loup C, Lacey CJ, Meunier B (1993) J Org Chem 58:2913–2917
36. Dubey L, Ryazanova O, Zozulya V, Fedoryak D, Dubey I (2011) Nucleosides Nucleotides Nucleic Acids 30(7–8):585–596
37. Mergny J-L, Phan A, Lacroix L (1998) FEBS Lett 435:74–78
38. Zozulya VN, Ryazanova OA, Voloshin IM, Glamazda AY, Karachevtsev VA (2010) J Fluoresc 20(3):695–702
39. Lakowicz JR (2006) Principles of fluorescence spectroscopy, 3rd edn. Springer, New York

40. Ryazanova OA, Voloshin IM, Makitruk VL, Zozulya VN, Karachevtsev VA (2007) Spectrochim Acta Part A: Mol Biomol Spectrosc 66(4–5):849–859
41. Seybold PG, Gouterman M (1969) J Mol Spectrosc 31:1–13
42. Gurinovich GP, Sevchenko AN, Soloviev KN (1963) Uspekhi Fizicheskih Nauk 79:173–234
43. Vergeldt FJ, Koehorst RBM, van Hoek A, Schaafsma TJ (1995) J Phys Chem 99:4397–4405
44. Kelly JM, Murphy MJ, McConnell DJ, OhUigin C (1985) Nucleic Acids Res 13(1):167–184
45. Schwarz G, Klose S, Balthasar W (1970) Eur J Biochem 12(3): 454–460
46. Schwarz G, Klose S, Balthasar W (1970) Eur J Biochem 12(3): 461–467
47. Zozulya VN, Fyodorov VF, Blagoi YP (1990) Stud Biophys 137: 17–28
48. Fiel RJ (1989) J Biomol Str Dyn 6:1259–1274